*J. Theoret. Biol.* (1969) **22,** 515–532

# Polyribosome Dynamics at Steady State

RICHARD GORDON†

*Department of Biophysics, University of Colorado Medical Center, Denver, Colorado, U.S.A.*

(*Received* 11 *July* 1968)

The Warner–Rich model for monocistronic polyribosomes is analyzed quantitatively by computer simulation. Its kinetic parameters may be directly related to those which are experimentally observable at steady state. Although simple cases can be solved exactly, it is found that computer simulation is a superior technique for polysomes of biologically significant size. The rate of protein synthesis, polysome distribution, ribosome gradient along the messenger, and distribution of nascent peptide lengths are given over the full range of variability of the free parameters for messenger RNA (mRNA) with a length of 150 codons. Measurements are suggested to test the validity of the Warner–Rich model, or certain of its predictions.

## 1. Introduction

Changes in polysome distributions are generally referred to the Warner–Rich model (Warner, Rich & Hall, 1962; Rich, Warner & Goodman, 1963; Wettstein, Staehelin & Noll, 1963). However, the properties of this model are, for the most part, only qualitatively understood, despite previous analytical incursions (Gerst & Levine, 1965; Zimmerman & Simha, 1965; Garrick, 1967; MacDonald, Gibbs & Pipkin, 1968). Thus we intend to examine the Warner–Rich model quantitatively, in such a manner that its kinetic parameters may be directly related to those which are experimentally observable. This study is restricted to monocistronic messenger RNA. We will discuss an approximate model of the Warner–Rich model in section 2, and treat simple cases of the exact model in section 3. It will be seen that the exact solution for polysomes carrying no more than two ribosomes is exceedingly cumbersome, and that larger polysomes are essentially intractable. The more fruitful and highly general approach of direct computer simulation is discussed in section 4, and a low activity approximation inspired by the simulation in section 5. Those parts which have high mathematical and low practical content have been set off by stars. A table of symbols has been provided as an Appendix.

† Current address: Department of Biological Sciences, Columbia University, New York City, N.Y., U.S.A.

## 2. Simple Models

Suppose that ribosomes of diameter $d$ codons attach at a free 5′ end of a messenger RNA (mRNA) at a specific rate $\alpha$, move from one codon to the next, if unhindered, at rate $\kappa$, and leave the 3′ end at rate $\beta$. If one of these processes is rate limiting, we can say that the steady-state rate of protein synthesis or flux $J = \min(\alpha, \beta, \kappa)$ ribosomes per unit time. This does not account for steric interference between the ribosomes, but since the latter could only decrease the flux, in general $J \leq \min(\alpha, \beta, \kappa)$. Thus a measured value of $J$ only sets a lower bound on $\alpha$, $\beta$ and $\kappa$. However, given the length $l$ of the mRNA in question, and the diameter $d$ of the ribosomes, the Warner–Rich model is fully determined. Thus it seems reasonable to ask whether $\alpha$, $\beta$ and $\kappa$ can be obtained from steady-state experimental data.

Consider a "deterministic" model, in which ribosomes arrive and depart from the ends stochastically, but move smoothly across the mRNA, until they encounter either a backup of ribosomes or the end of the message. If we take the limit $\alpha \to \infty$, with $\beta \geq \kappa$, ribosomes jump on as fast as room is available and thus proceed one immediately behind the other, so that $\bar{N} = N_{max}$, where $\bar{N}$ is the mean number of ribosomes on the message, and $N_{max}$ is its maximum capacity.

However, we expect the behaviour of a ribosome to be statistical in nature. At each codon it must wait a variable amount of time for the proper transfer RNA to come along and the various reactions involve activation energies, and thus transition probabilities. (In addition, these factors may vary from one codon to the next.) Therefore the ribosomes are in a real sense *diffusing* across the mRNA [even though they presumably cannot take backward steps; but see Sarabhai & Brenner (1967)]. We effectively have a case of one-dimensional diffusion with a saturating source ($\alpha \to \infty$) at one end, and a total sink at the other, so that there should be a "concentration" gradient across the mRNA. (The ribosomes will diffuse further and further apart as they proceed along the messenger.) Thus with $\beta \geq \kappa$ we expect $\bar{N} < N_{max}$, so that the "deterministic" model is qualitatively incorrect in this range. Its properties are not the means of a more chemically accurate stochastic model.

## 3. Stochastic Model

We shall assume then that each ribosome acts independently of the others, and moves statistically from one codon to the next, unless it is obstructed by a ribosome ahead, in which case it must stop and wait for that one to move. The model is a generalization of the lattice models for biological membranes considered by Hill & Kedem (1966), and we may try to apply similar methods for solving it. A solution consists of expressions for $J$ and

$P(N)$ in terms of $\alpha$, $\beta$, $\kappa$, $l$ and $d$. $P(N)$ is the probability that an mRNA holds $N$ ribosomes, which we shall call the polysome distribution. Experimental distributions, $E(N)$, based on optical density, are given by $E(N) = \text{const} \cdot NP(N)$, assuming that most of the absorption is due to the ribosomes. Thus experimental polysome distributions should be divided by $N$ and normalized for comparison with $P(N)$, or vice versa.

Let us consider a simple case, in which the messenger can hold no more than one ribosome, or $\alpha$ is so small that we rarely expect more than one on at a time.

*

The set of possible states and their numbering are shown in Fig. 1, in which, for the sake of illustration only, we have chosen $d = 3$ codons and

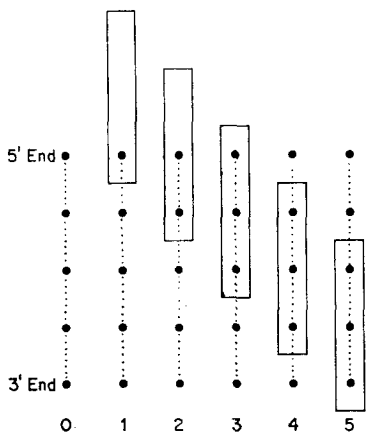


FIG. 1. Numbering scheme for the states of a polysome carrying no more than one ribosome. $l = 5$, $d = 3$. Each circle represents one codon.

$l = 5$ codons. In an ensemble or collection of such systems, if $P_i$ is the probability of finding a message in state $i$, we can write

$$\frac{\partial P_0}{\partial t} = \beta P_l - \alpha P_0 \tag{1}$$

$$\frac{\partial P_1}{\partial t} = \alpha P_0 - \kappa P_1$$

$$\frac{\partial P_i}{\partial t} = \kappa P_{i-1} - \kappa P_i \quad i = 2, \ldots, l-1$$

$$\frac{\partial P_l}{\partial t} = \kappa P_{l-1} - \beta P_l,$$

where $\sum_{i=0}^{l} P_i = 1$ (Hill & Kedem, 1966). Each expression on the right consists of a term describing the rate at which state $i$ appears, minus the rate at which it disappears. At steady state ($\partial P_i/\partial t = 0$) these linear equations may be solved to yield

$$P_i = (\alpha/\kappa)P_0 \quad i = 1,\ldots,l-1 \tag{2}$$
$$P_l = (\alpha/\beta)P_0$$

where

$$P_0 = [1+(l-1)\alpha/\kappa+\alpha/\beta]^{-1}$$

by the normalization.

* * *

We then obtain

$$\bar{N} = \sum_{i=1}^{l} P_i = 1-P_0 = \frac{\alpha}{\alpha+[(l-1)/\kappa+1/\beta]^{-1}} \tag{3}$$

which is of the form of a Langmuir or Michaelis–Menten adsorption isotherm (and in fact equals it for $l = 1$). The flux is $J = \alpha P_0$

$$= \bar{N}/[(l-1)/\kappa+1/\beta]$$

residues/unit time, so that

$$\alpha = J/(1-\bar{N}) \tag{4}$$
$$\beta = J/[\bar{N}-J(l-1)\ /\kappa].$$

An extra measurement is needed for $\kappa$. For instance, for large $l$, from $J = \alpha P_0$, we find $\kappa \approx Jl$. In general, if a messenger is long enough and its attached ribosomes are well-spaced and far from the ends, the rate of protein synthesis per ribosome over a short period of time should be an accurate measure of $\kappa$.

Note that experimental measurement of $\bar{N}$ requires measurement of $P(0)$, the fraction of messengers which have *no* ribosomes. $P(0)$ is rarely measured, but should be experimentally accessible. $P(1)$ is also required, which means that free ribosomes must be distinguished from monosomes. An indirect method for estimating $P(0)$ and $P(1)$ is discussed in section 4.

We will now demonstrate a method for obtaining the solution to the case in which mRNA can hold up to two ribosomes. [A similar problem is considered by Gerst & Levine (1965).]

*

The heart of our approach lies in our numbering system for the possible states of the polysome. If we number the codons consecutively from the 5′ end, we can use an ordered pair of numbers $(i, j)$, $j \geq i$, to indicate the

locations of the leading edges of the two ribosomes. If $i = 0$, $j > 0$, the messenger has only one ribosome. If $i = j = 0$, it is empty. For $i, j > 0$, note that $i \leq j-d$. If we define $(i, l+1) = (0, i)$, (or take the indices $\mathrm{mod}_{l+1}$, and then order them), then the states can be arranged in a triangular array, as shown in Table 1. An example of the scheme is shown in Fig. 2.

TABLE 1

*Connections between the states of a mRNA carrying up to two ribosomes, with the rate constants indicated*

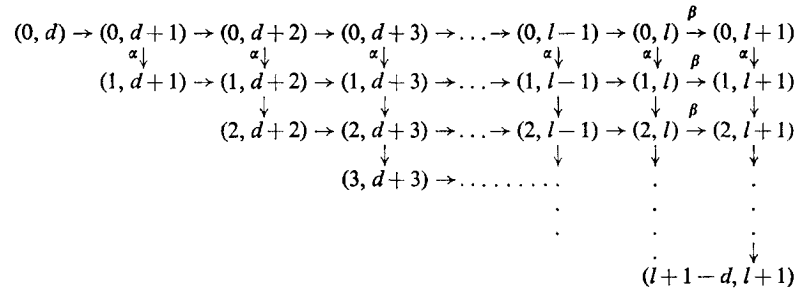


Unlabeled arrows correspond to the rate $\kappa$. Note that $\alpha$ appears only between the first and second rows, and $\beta$ only between the last two columns.

(Note that the actual location of the ribosome "active site" does not affect the dynamics of polysomes, because a different location would only result in a translation of the origin.)

Now let $P_{ij}$ represent the probability of state $(i, d+j)$, where $0 \leq i \leq l+1-d$ and $i \leq j \leq l+1-d$. (We have effectively translated the indices to the origin.) The normalization is given by

$$\sum_{i=0}^{l-d} \sum_{j=i}^{l-d} P_{ij} + \sum_{i=0}^{d-1} P_{i,l-d+1} = 1 \tag{5}$$

where we have accounted for the redundancy illustrated in Fig. 2. The formal steady-state solution is now quite straightforward, since every state may be solved for in terms of $P_{00}$, and $P_{00}$ evaluated from the normalization [equation (5)]. In particular, we have the recursive formulae:

* $$P_{0j} = \kappa P_{0,j-1}/(\alpha+\kappa) \quad j = 1, \ldots, l-d-1 \tag{6}$$

$$P_{0,l-d} = \kappa P_{0,l-d-1}/(\alpha+\beta)$$

$$P_{0,l-d+1} = \beta P_{0,l-d}/\alpha$$

$$P_{11} = \alpha P_{01}/\kappa$$

$$
\begin{aligned}
* \qquad P_{1j} &= (\alpha P_{0j} + \kappa P_{1,j-1})/(2\kappa) \qquad j = 2, \ldots, l-d-1 \\
P_{1,l-d} &= (\alpha P_{0,l-d} + \kappa P_{1,l-d-1})/(\beta+\kappa) \\
P_{1,l-d+1} &= (\alpha P_{0,l-d+1} + \beta P_{1,l-d})/\kappa \\
* \qquad P_{ii} &= P_{i-1,i} \qquad i = 2, \ldots, l-d-1 \\
* \qquad P_{ij} &= (1/2)(P_{i,j-1} + P_{i-1,j}) \qquad i = 2, \ldots, l-d-1; \\
&\qquad\qquad\qquad\qquad\qquad\qquad\qquad\qquad\qquad\qquad j = i+1, \ldots, l-d-1 \\
P_{i,l-d} &= \kappa(P_{i,l-d-1} + P_{i-1,l-d})/(\beta+\kappa) \qquad i = 2, \ldots, l-d-1 \\
P_{l-d,l-d} &= \kappa P_{l-d-1,l-d}/\beta \\
P_{i,l-d+1} &= (\beta P_{i,l-d} + \kappa P_{i-1,l-d+1})/\kappa \qquad i = 2, \ldots, d-1
\end{aligned}
$$

where the key equations are indicated by (*). In essence, except for the diagonals, each $P_{ij}$ is a weighted average of $P_{i,j-1}$ and $P_{i-1,j}$. The flux is

$$J = \alpha \sum_{j=1}^{l-d+1} P_{0j} = \beta \sum_{i=0}^{l-d} P_{i,l-d} \tag{7}$$

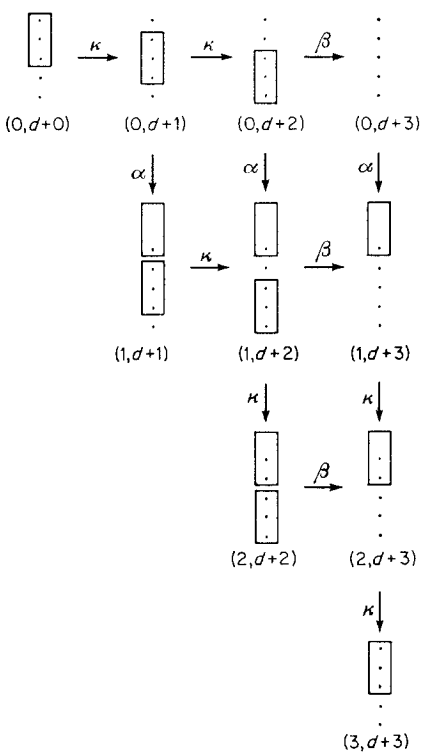


FIG. 2. An example of the scheme in Table 1, with $l = 5$, $d = 3$. Note that some states appear in both the first row and last column. [Just one in this case: $(0, d+0) = (3, d+3)$.]

residues/unit time, and the polysome distribution is

$$\begin{aligned} P(0) &= P_{0,l-d+1} \\ P(1) &= \sum_{j=0}^{l-d} P_{0j} + \sum_{i=1}^{d-1} P_{i,l-d+1} \\ P(2) &= \sum_{i=1}^{l-d} \sum_{j=i}^{l-d} P_{ij} \end{aligned} \tag{8}$$

with $\bar{N} = P(1)+2P(2)$.

We can solve immediately for

$$P_{0j} = [\kappa/(\alpha+\kappa)]^j P_{00} \qquad j = 1,\ldots,l-d-1. \tag{9}$$

If we now start solving for the $P_{1j}$ consecutively, we notice that if we define $R_{1j} = 2^{j-1}(\alpha+\kappa)^j P_{1j}$, then the $R_{1j}$ may be arranged in the form of Pascal's triangle, in which, moreover, each numerical coefficient $r_{jk}$ is the sum of the two above:

$$\begin{aligned} R_{11} &= 1\alpha \\ R_{12} &= 2\alpha\kappa + 1\alpha^2 \\ R_{13} &= 4\alpha\kappa^2 + 3\alpha^2\kappa + 1\alpha^3 \\ R_{14} &= 8\alpha\kappa^3 + 7\alpha^2\kappa^2 + 4\alpha^3\kappa + 1\alpha^4 \\ R_{15} &= 16\alpha\kappa^4 + 15\alpha^2\kappa^3 + 11\alpha^3\kappa^2 + 5\alpha^4\kappa + 1\alpha^5 \end{aligned} \tag{10}$$

Unlike Pascal's triangle, the left diagonal of equations (10) consists of powers of two. If we now subtract the corresponding binomial coefficient from each $r_{jk}$, we get the same array, just moved one left, so that

$$r_{j,k+1} = r_{jk} - \binom{j-1}{k-1}. \tag{11}$$

With the boundary condition $r_{j1} = 2^{j-1}$ we find

$$r_{jk} = 2^{j-1} - \sum_{i=0}^{k-1} \binom{j-1}{i-1} \tag{12}$$

$$P_{1j} = \frac{P_{00} \sum_{k=1}^{j} \left[ 2^{j-1} - \sum_{i=0}^{k-1} \binom{j-1}{i-1} \right] \alpha^k \kappa^{j-k}}{2^{j-1}(\alpha+\kappa)^j} \qquad j = 1,\ldots,l-d-1$$

$P_{1,l-d}$ and $P_{1,l-d+1}$ can now readily be calculated.

It is apparent from Table 1 that the rest of the $P_{ij}$ are linear combinations of the $P_{1j}$. Moreover, except for the last two columns, the rate constants do not enter, so that the coefficients are pure numbers, $c_{ijk}$, where $P_{ij} = \sum_{k=2}^{j} c_{ijk} P_{1k}$, $= (c_{ij2}, c_{ij3}, \ldots)$ in vector notation ($c_{ijk} = 0$ for $k > j$) (Ulam, 1968). In

particular, $P_{12} = (1, 0, 0, \ldots)$, $P_{13} = (0, 1, 0, \ldots)$, etc. If we start writing these vectors out according to $P_{ii} = P_{i-1,i}$, $P_{ij} = (1/2)(P_{i,j-1} + P_{i-1,j})$, using vector addition, we notice that $c_{ijk} = r_{ijk}/2^{i+j-k-1}$, where $r_{ijk}$ is an integer (Table 2). The $r_{ijk}$ conform to the recursion relations

$$\begin{aligned} r_{iik} &= 2r_{i-1,i,k} \\ r_{ijk} &= r_{i-1,j,k} + r_{i,j-1,k} \qquad j > i \end{aligned} \tag{13}$$

TABLE 2

*Beginning of the table of vectors* $c_{ijk}$, $k = 2, 3, \ldots$

| $i$ | $j$: 2 | 3 | 4 |
|---|---|---|---|
| 1 | 1, 0, 0, 0, ... | 0, 1, 0, 0, ... | 0, 0, 1, 0, 0, ... ... |
| 2 | $\frac{2}{2}$, 0, 0, 0, ... | $\frac{2}{4}$, $\frac{1}{2}$, 0, 0, ... | $\frac{2}{8}$, $\frac{1}{4}$, $\frac{1}{2}$, 0, 0, ... ... |
| 3 | | $\frac{4}{8}$, $\frac{2}{4}$, 0, 0, ... | $\frac{6}{16}$, $\frac{3}{8}$, $\frac{1}{4}$, 0, 0, ... ... |
| 4 | | | $\frac{12}{32}$, $\frac{6}{16}$, $\frac{2}{8}$, 0, 0, ... ... |

If we arrange the $r_{ijk}$ for given $j$ in a diamond, we obtain, for instance, for $j = 7$, $i \geq 2$

$$\begin{array}{ccccccccccccc} & & & & & & 1 & & & & & & \\ & & & & & 1 & & 1 & & & & & \\ & & & k\nearrow & & 1 & & 2 & & 1 & & & \\ & & & & 1 & & 3 & & 3 & & 1 & & \\ & & & 1 & & 4 & & 6 & & 4 & & 1 & \\ & & 2 & & 6 & & 11 & & 11 & & 6 & & 2 \\ & & & 12 & & 21 & & 26 & & 21 & & 12 & \\ & & & & 42 & & 56 & & 56 & & 42 & & \\ & & & i\searrow & & 112 & & 126 & & 112 & & & \\ & & & & & & 252 & & 252 & & & & \\ & & & & & & & 504 & & & & & \end{array}$$

The top elements of this array are just the binomial coefficients, and if we subtract the corresponding elements of Pascal's triangle from it, we obtain as remainders

$$
\begin{array}{ccccccccccccc}
 & & & & & & 0 & & & & & & \\
 & & & & & 0 & & 0 & & & & & \\
 & & & & 0 & & 0 & & 0 & & & & \\
 & & & 0 & & 0 & & 0 & & 0 & & & \\
 & & 0 & & 0 & & 0 & & 0 & & 0 & & \\
 & 1 & & 1 & & 1 & & 1 & & 1 & & 1 & \\
 & & 6 & & 6 & & 6 & & 6 & & 6 & & \\
 & & & 21 & & 21 & & 21 & & 21 & & & \\
 & & & & 56 & & 56 & & 56 & & & & \\
 & & & & & 126 & & 126 & & & & & \\
 & & & & & & 252 & & & & & &
\end{array}
$$

which are recognizable binomial coefficients. Thus each $r_{ijk}$ is the sum of two binomial coefficients. In particular, we arrive at

$$P_{ij} = (\tfrac{1}{2})^{i+j} \sum_{k=2}^{j} 2^{k+1} \left[ \binom{i+j-k-2}{i-2} + \binom{i+j-k-2}{i-k} \right] P_{1k} \qquad (14)$$

$$i = 2, \ldots, l-d-1; j = i, \ldots, l-d-1$$

and the last two columns of Table 1 can now be calculated. From the normalization [equation (5)], we find that $P_{00}$ consists of the ratio of two polynomials approximately of order $2(l-d)$, (up to $l-d$ in $\alpha$ and $\beta$, and $2(l-d)$ in $\kappa$). The solution is rather cumbersome and difficult to work with. Its inversion to obtain $\alpha$ and $\beta$ as functions of $J$ and $\bar{N}$ requires numerical methods. Moreover, the extension of this method to polysomes with up to three ribosomes requires a three-dimensional analog of Table 1, which has two pyramids, and does not allow for direct solution of all states in terms of $(0, 0, d)$. (There are two "backwards" loops necessitating the solution of two simultaneous equations before normalization is possible.) For more than three ribosomes, the exact solution is even less tractable. Thus we turn to a less exact but perfectly general approach to polysome dynamics.

* * *

## 4. Computer Simulation of the Steady State

We represent the codons of an mRNA by a sequence of computer "words" or memory units (designated in a FORTRAN program), which are given the value $k$ if they are covered by the $k$th ribosome on the message, and the value 0 if uncovered. In addition, a list of the current positions of the ribosomes is kept, as is an indicator of whether or not the forward motion of each is blocked. We define an event as attachment of a new ribosome

at the 5′ end, movement of any ribosome by one codon, or detachment from the 3′ end. Each event occurs at a specific rate, and that event which occurs next in a given program cycle is chosen at random according to the relative rates, using the Monte-Carlo technique of Gordon (1968).

We choose our time unit to be the mean time it takes an unhindered ribosome to move one codon, ($1/\kappa = 1$), and measure the polysome distribution, mean number of ribosomes, and flux in residues/unit time for given values of $\alpha$ and $\beta$. An option is also provided for measuring the mean ribosome "gradient" across the messenger and the distribution of nascent protein lengths. Without the latter feature, on a Control Data 6400 computer, the program executes at $\sim 2500$ events/sec, or 10 to 100 times faster than real polysomes. In order to assure that steady state has been attained, the runs are started with the mRNA alternately empty and full of ribosomes, and at least the first $l^2/d$ events are discarded. Steady state measurements are made from at least the next $5l^2/d$ ensuing events.

The diameter of ribosomes in electron microscope preparations has been found to be 200 to 230 Å (Dibble, 1964; Malkin & Rich, 1967). However, small-angle X-ray scattering (Dibble, 1964) and diffusion coefficient measurements (Wolfe & Kay, 1967) suggest a wet diameter of 340 to 370 Å. Dibble (1964) proposes that "the ribosome is like a sponge, or perhaps a spherical 'tree' or some other open structure". If we assume the average nucleotide spacing in mRNA is 3·4 Å (Rich *et al.*, 1963), then the observed diameters correspond to a range of 20 to 36 codons. Thus the value $d = 27$ codons, recommended to us by C. T. MacDonald (1967, personal communication), should be a reasonable estimate of the *hard core* diameter of ribosomes, and this is the value we have used in the simulation. [There are species variations: for instance, compare Dibble (1964) with Bohn, Farnsworth & Dibble (1967).]

The following observations and conclusions were drawn from the simulation of polyribosomes at steady state:

(1) Comparison of the simulation with the exact solution for up to two ribosomes.

*

A short computer program was written which evaluated the recursive equations (6) directly for given values of $\alpha$ and $\beta$, with $\kappa = 1$, $d = 27$, $l = 54$, $P_{00} = 1$ momentarily. The $P_{ij}$ were then normalized by equation (5), and $J$, $P(N)$, and $\bar{N}$ calculated [equations (7) and (8)]. The redundancy of two states in the $P_{ij}$ array (as in Fig. 2) and equation (7) provided a check on the calculation.

* * *

The detailed agreement between the exact calculation and the simulation (Fig. 3) indicates that the computer program probably contains no errors, and illustrates the statistical reliability of the simulation.

(2) Saturation. As we anticipated in section 2, when $\beta \geq \kappa$ the mean polysome size is always less than $N_{max}$, as exemplified in Fig. 4, in which we plot $\bar{n} = \bar{N}/N_{max}$ vs. $\log_{10} \alpha$ (which is proportional to the chemical potential of the free ribosomes). There are two distinguishable results of the "independent" statistical motion of the ribosomes. Not only is $\bar{N} < N_{max}$, but also each ribosome moves at a mean velocity significantly less than that of an unhindered ribosome. Relative to an ideal situation, in which the ribosomes do not interfere with one another (such as the "deterministic" model, with $\beta \geq \kappa$), the efficiency of long messengers is only 69% (see Fig. 5). (However, certain shorter lengths are significantly more efficient in their utilization of ribosomes.) Although the number of ribosomes increases for

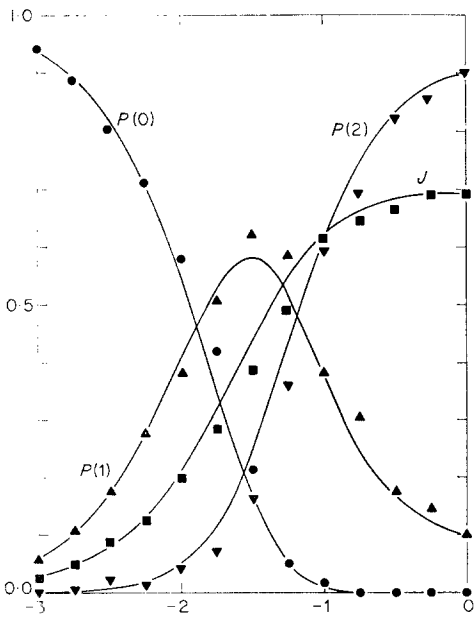


FIG. 3

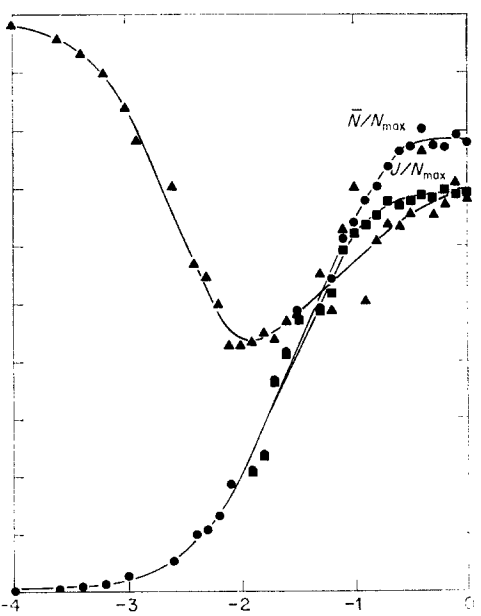


FIG. 4

FIG. 3. A comparison between the simulation and an exact calculation. The lines are based on equations (6) to (8). $l = 54$, $\beta = 10^{-1}$. The first 200 events were rejected and the next 700 measured.

FIG. 4. A typical non-equilibrium adsorption isotherm for a polysome of length $l = 150$ codons, with $\beta = 10^{0}$. The first 1000 events were rejected and the next 5000 measured. (—●—●—) $\bar{n} = \bar{N}/N_{max}$, mean occupation; (—■—■—) $J/N_{max}$, flux; (—▲—▲—) $\delta$, normalized deviation, equation (15).

$\beta < \kappa$, the total flux never exceeds the value shown in Fig. 5 for a given $l$.

(3) All polysome distributions for a given $l$ are single-peaked (see Fig. 8). Minor exceptions in the polysome distributions obtained from the simulation could be attributed to runs which were not sufficiently long to give the true steady-state distribution. (We are simulating a single mRNA, so that fluctuations can be quite large.) One consequence of this property is that it may be possible to extrapolate an observed distribution, by taking the best fit to a simulated distribution, in order to obtain $P(1)$ and $P(0)$, and

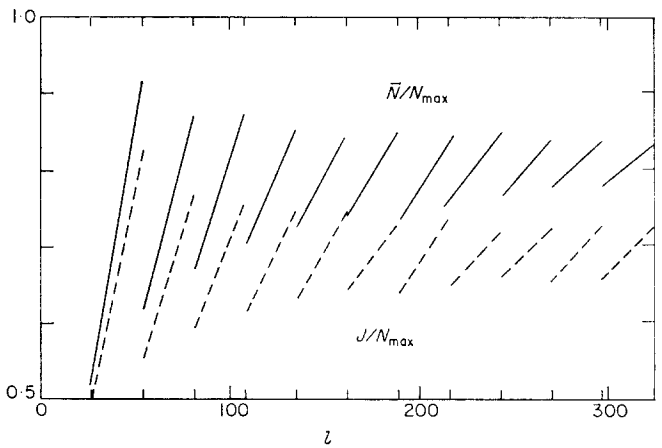


FIG. 5. Mean occupation, $\bar{n} = \bar{N}/N_{max}$, (———) and normalized flux, $J/N_{max}$, (– – – –) as a function of the length $l$ of the mRNA. The space between the small tick marks equals one ribosome diameter (27 codons). The extrapolated midpoints are $0{\cdot}80_5$ and 0·69, respectively.

thus $\bar{N}$. Another is that experimental distributions which are not single peaked probably represent preparations in which the mRNA has been degraded or is heterogeneous.

(4) Simultaneous determination of $\alpha$ and $\beta$. Runs were made with many different values of $\alpha$ and $\beta$ for $l = 150$. The resulting values of $\bar{N}$ and $J$ were plotted in various ways and smoothed and interpolated by hand. As a result, we are able to draw lines of equal $\bar{N}$ and lines of equal flux $J$ on a graph of $\beta$ vs. $\alpha$ (Fig. 6). From experimentally determined $\bar{N}$ and $J$, one need only find the intersection of the corresponding lines, to read off $\alpha$ and $\beta$ directly. Similar graphs could be constructed for other values of $l$.

In Fig. 7 we have also plotted the normalized deviation from a flat polysome distribution, given by

$$\delta = \left\{ \sum_{N=0}^{\eta} [P(N) - 1/(\eta+1)]^2 \right\}^{1/2} \Big/ \delta_{\max} \tag{15}$$

where $\eta = N_{\max}$ and

$$\delta_{\max}^2 = [1 - 1/(\eta+1)]^2 + \eta[1/(\eta+1)]^2$$

is the maximum possible deviation from $P(N) = 1/(\eta+1)$. $\delta$ is analogous to a standard deviation. It may be used as a check on a determination of $\alpha$ and $\beta$, or as an independent variable.

Figure 8 shows polysome distributions for a few values of $\alpha/\kappa$ and $\beta/\kappa$. From these, or from $\delta$ in Fig. 7, we can learn, for instance, that if we decrease $\kappa$ for fixed $\alpha$ and $\beta$, $\alpha \approx \beta$, the polysome distribution changes from a flat one to one which is moderately peaked. If initially $\bar{n} < 0{\cdot}8$, it will increase as $\kappa$ decreases (Fig. 6). For $\bar{n} > 0{\cdot}8$ initially, the reverse will occur. Such considerations may make it possible to distinguish between the two modes of action of $4 \times 10^{-6}$ M-cycloheximide on reticulocyte polysomes which have been proposed by Godchaux, Adamson & Herbert (1967). They

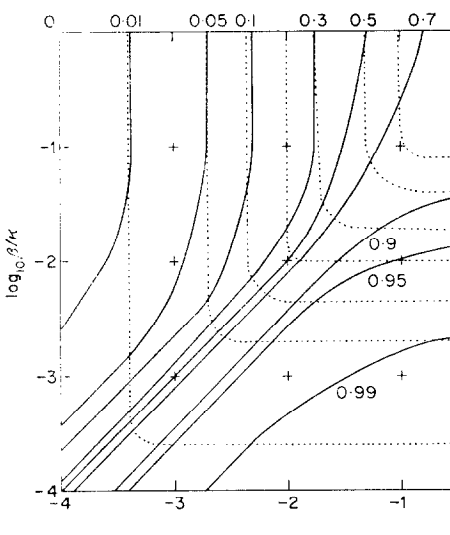


FIG. 6

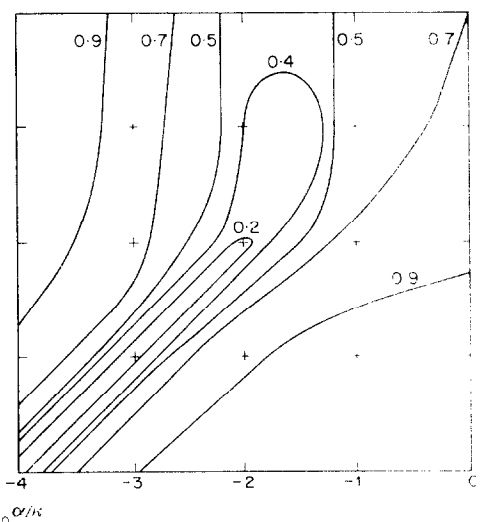


FIG. 7

FIG. 6. Lines of constant flux, $J/(\kappa N_{\max})$, (· · · · ·, labeled inside to the right), and lines of constant $\bar{N}/N_{\max}$, (———, labeled outside and in the middle), for $l = 150$. The parallel lines in the lower left-hand corner are based on solutions of equation (21). This figure may be used to obtain $\alpha$ and $\beta$ from experimentally determined values of the flux and mean occupation. Note $N_{\max} = 6$, $l = 150$ in Figs 6 to 10.

FIG. 7. The normalized deviation, $\delta$ (defined in equation (15)) as a function of $\alpha$ and $\beta$.

FIG. 8

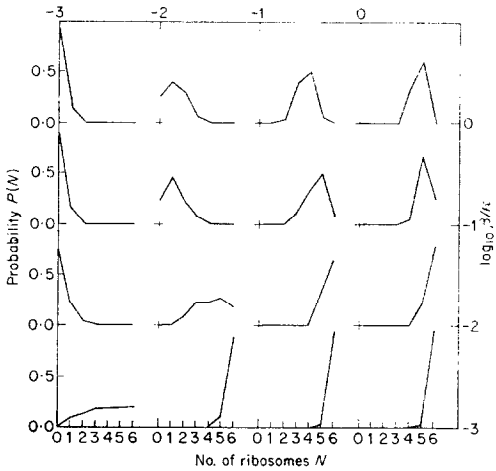


FIG. 9

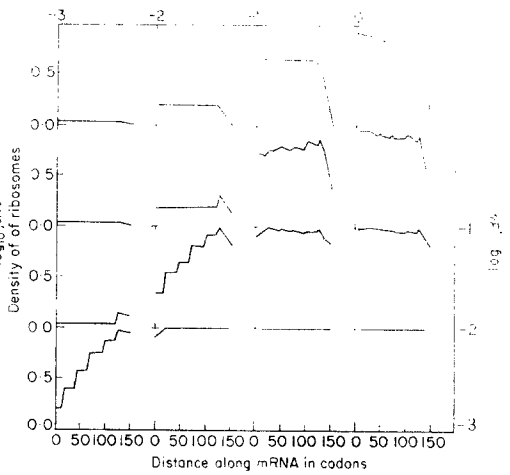


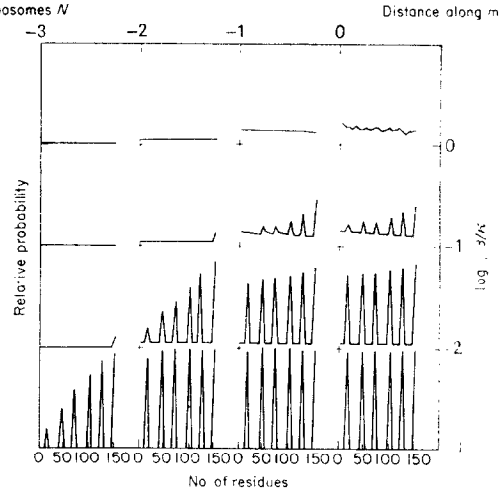


FIG. 10

FIGS. 8 to 10. The polysome distributions, ribosome gradients, and relative distributions of the nascent peptide lengths, respectively, for 16 individual runs of the simulation, illustrated as "graphs of graphs". The probabilities for every 5 successive codons were averaged to give the nascent peptide distributions in Fig. 10. The actual distributions may have sharper peaks. In each run the first 1000 events were rejected and the next 5000 measured.

suggested that the lowered rate of protein synthesis, accompanied by a shifted polysome distribution, was due either to a decrease in the detachment rate ($\beta$) or a decreased rate of "addition of amino acids to the nascent polypeptide chains" ($\kappa$).

## 5. A Low Activity Approximation

Some rather odd, uphill, step-like gradients across the mRNA were observed in the computer simulation (Fig. 9), for which the following explanation was found. When the traversal time of a ribosome is short compared to the mean arrival and departure times, $l/\kappa \ll \min(1/\alpha, 1/\beta)$, the polysome becomes a simple queue of finite capacity. Ribosomes arrive on occasion and move (relatively) rapidly to the pileup at the end. Every once in a while the end ribosome jumps off, and the others rapidly shift over. All the intermediate states can be ignored, so that the polysome distribution itself, $P(N)$, becomes an adequate description of the important states of the system.

We may then write:

$$\begin{aligned}
\frac{\partial P(0)}{\partial t} &= -\alpha P(0)+\beta P(1) \\
\frac{\partial P(i)}{\partial t} &= \alpha P(i-1)-(\alpha+\beta)P(i)+\beta P(i+1) \qquad i = 1,\ldots,\eta-1 \\
\frac{\partial P(\eta)}{\partial t} &= \alpha P(\eta-1)-\beta P(\eta).
\end{aligned} \tag{16}$$

At steady state, if we assume that $P(i) = (\alpha/\beta)^i P(0)$, then $P(i+1)$ is of the same form. Since the formula is true for $P(0)$, by finite induction (Birkhoff & MacLane, 1953) it is true for all $i$. By normalization we obtain $P(0)$ and thus

$$P(i) = r^i(1-r)/(1-r^{\eta+1}) \qquad i = 0, 1, \ldots, \eta, \tag{17}$$

where $r = \alpha/\beta$. In addition

$$J = \beta \sum_{i=1}^{\eta} P(i) = \beta(1-P(0)) = \alpha(1-r^\eta)/(1-r^{\eta+1}) \tag{18}$$

$$\bar{N} = \frac{\sum_{i=0}^{\eta} iP(i)}{\sum_{i=0}^{\eta} P(i)} = \frac{\sum_{i=0}^{\eta} ir^i}{\sum_{i=0}^{\eta} r^i} = \frac{r[1-(\eta+1)r^\eta+\eta r^{\eta+1}]}{(1-r)(1-r^{\eta+1})}. \tag{19}$$

Equations (17) to (19) are valid for $\alpha = \beta$ if L'Hospital's rule (Johnson & Kiokemeister, 1959) is applied:

$$\begin{aligned}
P(i)_{\alpha=\beta} &= 1/(\eta+1) \\
J_{\alpha=\beta} &= \alpha\eta/(\eta+1) \\
\bar{N}_{\alpha=\beta} &= \eta/2.
\end{aligned} \tag{20}$$

$P(i)_{\alpha=\beta}$ is the perfectly flat polysome distribution for which $\delta = 0$.

Inversion may be accomplished by finding the unique positive root $r(\bar{N})$ of

$$\sum_{i=0}^{\eta} (i-\bar{N})r^i = 0 \tag{21}$$

(derived from equation (19)) and calculating:

$$\alpha = J[1-(r(\bar{N}))^{\eta+1}]/[1-(r(\bar{N}))^{\eta}] \tag{22}$$
$$\beta = \alpha/r(\bar{N}).$$

* * *

There are two physical consequences of low activity. As noted, one is that the mean ribosome gradient across the mRNA is a step function, monotonically *increasing* from the attachment end (contrary to the more normal gradient for high $\alpha$ and $\beta$). This is because the heights of the steps are $P(\eta)$, $P(\eta)+P(\eta-1)$, $P(\eta)+P(\eta-1)+P(\eta-2)$, etc. Second, because of the discrete positions of the ribosomes, there will also be a discrete distribution of nascent peptide lengths, the unit difference being $d$ peptides. This property could possibly be used to measure the "hard core" diameter of ribosomes. In conjunction with a calculation or measurement of the elasticity of a ribosome, the hard core diameter could yield an estimate for the force with which the ribosome-messenger ratchet moves forward. Such gradients and peptide distributions are illustrated in Figs 9 and 10.

From Fig. 9 we may note that some conditions do not lead to flat ribosome gradients across the mRNA. Thus the assumption of flat gradients, made by Kuff & Roberts (1967) in a test of the Warner–Rich model, may have been incorrect.

*

An interesting feature of the polysome system from a statistical mechanics point of view is that in the limit of infinite length this one-dimensional system has a (non-equilibrium) phase transition. From equation (19):

$$\lim_{\eta\to\infty} \frac{\bar{N}(r)}{\eta} = \begin{cases} 0 & r < 1 \\ \frac{1}{2} & r = 1 \\ 1 & r > 1 \end{cases} \tag{23}$$

$\bar{N}(r)$ exhibits a common symmetry (Hill, 1960):

$$\eta - \bar{N}(r) = \bar{N}(1/r). \tag{24}$$

* * *

## 6. Discussion

Computer simulation proved to be a superior technique for investigating polyribosome dynamics over the full range of the free parameters. In addition it was an excellent heuristic device, in that simulated results suggested the low activity approximation. With minor modifications, the same computer program could be used to calculate transients.

As simple as the Warner–Rich model is, we have shown that computer simulation is necessary to attain a quantitative understanding of its behavior. Approximations are models of models, two steps removed from reality. They can even be qualitatively wrong. As the details of protein synthesis become better known, and more complex models are devised, rapid and flexible simulation of these models on computers will be necessary for an accurate understanding of their dynamic properties, and for comparison with experimental results.

The author would like to thank Victor A. Fried for suggesting the problem, and Mr Fried and Drs Melvin Averner, Jack B. Carmichael, David Cox, and John R. Sadler for suggesting improvements in the manuscript.

Preliminary computing was supported by a grant to Prof. Edward Herbert from the National Institutes of Health, and a National Science Foundation Science Development grant to the University of Oregon Computing Center. Computing was continued with a grant from the University of Colorado Computer Center.

This work is from the Eleanor Roosevelt Institute for Cancer Research and the Department of Biophysics (contribution no. 336), University of Colorado Medical Center, Denver, Colorado. Investigation was further aided by a grant (5 P01 HD02080) from the National Institutes of Health, U.S. Public Health Service.

Copies of the computer program are available upon request.

## REFERENCES

BIRKHOFF, G. & MACLANE, S. (1953). "A Survey of Modern Algebra", Ch. 1. New York: MacMillan Co.

BOHN, T. S., FARNSWORTH, R. K. & DIBBLE, W. E. (1967). *Biochim. biophys. Acta*, **138**, 212.

DIBBLE, W. E. (1964). *J. Ultrastruct. Res.* **11**, 363.

GARRICK, M. D. (1967). *J. Theoret. Biol.* **17**, 19.

GERST, I. & LEVINE, S. N. (1965). *J. Theoret. Biol.* **9**, 16.

GODCHAUX, III, W., ADAMSON, S. D. & HERBERT, E. (1967). *J. molec. Biol.* **27**, 57.

GORDON, R. (1968). *J. chem. Phys.* **49**, 570.

HILL, T. L. (1960). "An Introduction to Statistical Thermodynamics", Section 14–1. Reading, Mass.: Addison-Wesley.

HILL, T. L. & KEDEM, O. (1966). *J. Theoret. Biol.* **10**, 399.

JOHNSON, R. E. & KIOKEMEISTER, F. L. (1959). "Calculus", Ch. 13. Boston: Allyn & Bacon, Inc.

KUFF, E. L. & ROBERTS, N. E. (1967). *J. molec. Biol.* **26**, 211.

MACDONALD, C. T., GIBBS, J. H. & PIPKIN, A. C. (1968). *Biopolymers*, **6**, 1.

MALKIN, L. I. & RICH, A. (1967). *J. molec. Biol.* **26**, 329.

RICH, A., WARNER, J. R. & GOODMAN, H. M. (1963). *Cold Spring Harb. Symp. quant. Biol.* **28,** 269.
SARABHAI, A. & BRENNER, S. (1967). *J. molec. Biol.* **27,** 145.
ULAM, S. M. (1968). *SIAM Rev.* **10,** 258.
WARNER, J. R., RICH, A. & HALL, C. E. (1962). *Science, N.Y.* **138,** 1399.
WETTSTEIN, F. O., STAEHELIN, T. & NOLL, H. (1963). *Nature, Lond.* **197,** 430.
WOLFE, F. H. & KAY, C. M. (1967). *Biochemistry,* **6,** 2853.
ZIMMERMAN, J. M. & SIMHA, R. (1965). *J. Theoret. Biol.* **9,** 156.

## Appendix

### *Symbols*

$\alpha$ rate at which ribosomes attach at the free 5′ end of an mRNA

$\beta$ rate at which ribosomes detach from the 3′ end

$\kappa$ rate at which unhindered ribosomes hop from one codon to the next

$r$ $= \alpha/\beta$

$J$ flux of ribosomes or rate of protein synthesis, measured in either ribosomes/unit time or residues/unit time

$d$ hard core diameter of a ribosome, in units equal to the length of one codon

$\bar{N}$ mean number of ribosomes on an mRNA

$N_{\max}$ maximum number of ribosomes which an mRNA of a given length can hold

$\bar{n}$ $= \bar{N}/N_{\max}$

$\eta$ $= N_{\max}$

$l$ length of an mRNA in codons

$P(N)$ probability that an mRNA holds $N$ ribosomes (our "polysome distribution")

$P_i$ or $P_{i,j}$ the probability of a particular *state* of a polysome

$E(N)$ experimentally observed polysome distribution measured by ultraviolet absorption

$\delta$ normalized deviation from a flat polysome distribution
$P(N) = 1/(\eta+1)$